Colossal magnetoresistance of $La_{0.35}Nd_{0.35}Sr_{0.3}MnO_3$ epitaxial thin film on (001)$ZrO_2(Y_2O_3)$ substrate over a wide temperature range



2001 J. Phys.: Condens. Matter 13 5901

(http://iopscience.iop.org/0953-8984/13/26/305)

INSTITUTE OF PHYSICS PUBLISHING JOURNAL OF PHYSICS: CONDENSED MATTER

J. Phys.: Condens. Matter **13** (2001) 5901–5916 www.iop.org/Journals/cm PII: S0953-8984(01)22658-7

# Colossal magnetoresistance of $La_{0.35}Nd_{0.35}Sr_{0.3}MnO_3$ epitaxial thin film on (001)$ZrO_2(Y_2O_3)$ substrate over a wide temperature range

**L I Koroleva[1,5], A I Abramovich[1], A V Michurin[1], O Yu Gorbenko[2], I E Graboy[2], A R Kaul[2], R Szymczak[3], S Dyeyev[3] and H W Zandbergen[4]**

[1] Physics Department, Moscow State University, 119899 Moscow, Russia
[2] Chemistry Department, Moscow State University, 119899 Moscow, Russia
[3] Institute of Physics, Polish Academy of Sciences, Warsaw, 02-668, Poland
[4] National Centre for HREM, TU Delft, Rotterdamsweg 137, 2628AL Delft, The Netherlands

E-mail: koroleva@ofef343.phys.msu.su

Received 8 March 2001, in final form 11 May 2001

**Abstract**

Colossal negative magnetoresistance is found over a wide range of temperatures below the Curie point $T_C \approx 240$ K in an epitaxial $La_{0.35}Nd_{0.35}Sr_{0.3}MnO_3$ film on a single-crystal (001)$ZrO_2(Y_2O_3)$ wafer substrate. Isotherms of the magnetoresistance of this film reveal that its absolute value increases with the field, abruptly in the technical magnetization range and almost linearly in stronger fields. For three epitaxial films of the same composition on (001)$LaAlO_3$, (001)$SrTiO_3$, and (001)MgO substrates, colossal magnetoresistance only occurred near $T_C \approx 240$ K and at $T < T_C$ it increased weakly, almost linearly with the field. In the film on $ZrO_2(Y_2O_3)$ substrate the electrical resistivity was almost 1.5 orders of magnitude higher than that in the other three films. It is shown that this increase is attributable to the electrical resistance of the interfaces between microregions having four types of crystallographic orientation, while the magnetoresistance in the region before technical saturation of the magnetization is attributable to tunnelling of polarized carriers across these interfaces which coincide with the domain walls (in the other three films there is one type of crystallographic orientation). The reduced magnetic moment observed for all four samples, which is only 46% of the pure spin value, can be attributed to the existence of magnetically disordered microregions which originate from the large thickness of the domain walls which is greater than the size of the crystallographic microregions and is of the same order as the film thickness. The colossal magnetoresistance near $T_C$ and the low-temperature magnetoresistance in fields exceeding the technical saturation level can be attributed to the existence of strong s–d exchange which is responsible for a steep drop in the mobility of the carriers (holes) and their partial localization at levels near the top of the valence band. Under the action of the magnetic field the carrier mobility increases and they become delocalized from these levels.

[5] Author to whom any correspondence should be addressed. Fax: +7-095-932-8820.

  

## 1. Introduction

Although manganites having a perovskite structure have been known of for some time [1, 2], they have attracted a new wave of interest since 1995 following the observation of colossal negative magnetoresistance in thin films of various compositions at room temperature. These compositions can be used as the basis for developing various sensors. The colossal magnetoresistance in these compounds is observed in a narrow temperature range near the Curie point $T_C$. Since any device should have stable characteristics in the operating temperature range, for practical applications it is important to extend the range of temperatures in which colossal magnetoresistance could occur. It has been noted in various studies using both bulk and thin-film polycrystalline samples that a high magnetoresistance is observed at low temperatures and the peak in the curve of the magnetoresistance magnitude as a function of temperature broadens substantially near $T_C$ [3–17]. In weak magnetic fields before technical saturation of the magnetization was achieved, the colossal magnetoresistance was ascribed to spin-polarized tunnelling between granules [9] or scattering of carriers within domain walls which generally coincide with grain boundaries [4]. However, in some of these studies it was noted that in stronger magnetic fields the magnetoresistance magnitude continued to increase almost linearly with the field. A similar almost linear increase in the magnetoresistance magnitude at low temperatures was also observed in single-crystal samples. This phenomenon has not been explained.

In an earlier study we observed that $La_{0.85}Sr_{0.15}MnO_3$ film on an (001)$ZrO_2(Y_2O_3)$ single-crystal wafer substrate exhibits colossal magnetoresistance over a wider temperature range than films on a (001)$LaAlO_3$ single-crystal wafer substrate [18]. The aim of the present study was to determine whether colossal magnetoresistance could be observed over a wide temperature range in epitaxial manganite films. For this purpose we studied thin epitaxial films of $La_{0.35}Nd_{0.35}Sr_{0.3}MnO_3$ on substrates of (001)$SrTiO_3$, (001)$LaAlO_3$, (001)MgO, and (001)$ZrO_2(Y_2O_3)$ single-crystal wafers. This composition is attractive because it is almost at the morphotropic boundary between the orthorhombic ($Pnma$) and rhombohedral ($R3c$) structures. Thus, the distortions of the perovskite structure are so small that they cannot be detected by x-ray analysis. The lattice strain typical of manganite films is very small in these films at thickness higher than 300–400 nm and need not be taken into account when discussing the reasons for the colossal magnetoresistance at low temperatures.

We established that the film on (001)$ZrO_2(Y_2O_3)$ exhibits colossal magnetoresistance not only near $T_C$ but also at $T < T_C$ as far as 4.2 K.

Another aim of the present study was to describe the physical reasons for the colossal magnetoresistance observed by us over a wide range of temperature in epitaxial film on (001)$ZrO_2(Y_2O_3)$ wafer and also for the increase in the magnetoresistance magnitude with field at $T < T_C$ observed in all the films described above in magnetic fields exceeding the technical magnetization saturation level.

## 2. Preparation of thin films and experimental techniques

The films were prepared by metallo-organic chemical vapour deposition (MOCVD) using an aerosol source of vapour of the metallo-organic compounds. A powder mixture of the metallo-organic precursors ($La(thd)_3$, $Nd(thd)_3$, $Sr(thd)_2$, $Mn(thd)_3$, where thd = tetramethylheptandion-3, 5-ate) was introduced stepwise into the evaporator and then the precursor vapour was transported by argon flow into the reactor in parallel to the oxygen flow. A cold-wall MOCVD reactor with a downstream stagnation flow geometry was used. The process

parameters are listed in table 1. After the deposition all films were annealed for 0.5 h in an oxygen flow at the pressure of 1 bar.

The composition and structure of the films prepared were characterized by x-ray diffraction (XRD), scanning electron microscopy (SEM) with energy-dispersive x-ray analysis (EDX), and high-resolution electron microscopy (HREM) performed with the four-circle diffractometer Siemens D-5000 (Cu K$\alpha$ radiation, secondary graphite monochromator). The SEM was accomplished with a CamScan electron microscope equipped with an EDX system for quantitative chemical analysis. The HREM study of the films on MgO, $SrTiO_3$, and $LaAlO_3$ in the cross-section geometry was performed with the use of a Philips CM30UT electron microscope operating at 300 kV. The thicknesses of the films were measured with a Talystep profilometer over the chemically etched step in the film.

**Table 1.** Deposition process parameters.

| Parameters | Values |
|---|---|
| Deposition temperature | 750 °C |
| Precursor evaporation temperature | 260 °C |
| Total pressure | 6.5 mbar |
| Argon flow | 30 l $h^{-1}$ |
| Oxygen flow | 15 l $h^{-1}$ |
| Deposition rate | 1 $\mu$m $h^{-1}$ |
| Film thickness | 400–550 nm |
| Substrates | (001)$SrTiO_3$, (001)MgO, (001)$ZrO_2(Y_2O_3)$, (001)$LaAlO_3$ |

The magnetization of the thin films was determined using a SQUID magnetometer and the electrical resistivity was determined by a four-probe method. The magnetoresistance was measured in the plane of the film when the current through the film was parallel to the magnetic field $\boldsymbol{H}$.

## 3. Experimental results

### *3.1. Crystallographic properties*

*3.1.1. X-ray diffraction.* According to $\theta$–$2\theta$ scans, the films on $SrTiO_3$, MgO, and $LaAlO_3$ were (001) oriented and the films on $ZrO_2(Y_2O_3)$ were (110) oriented (figure 1). These film orientations are typical for perovskite manganites [19]. The unusual orientation of the film on $ZrO_2(Y_2O_3)$ can be explained by an electrostatic model. The in-plane orientation was characterized by $\varphi$-scans. The films on $SrTiO_3$, MgO, and $LaAlO_3$ reveal an epitaxial alignment with the substrate known as the 'cube-on-cube' growth mode. The films on $ZrO_2(Y_2O_3)$ demonstrate a definite in-plane orientation too, but a more complex one. The volume diagonals of the perovskite cubes were found to be aligned along the face diagonal of the fluorite cube of the $ZrO_2(Y_2O_3)$ structure. There are four equivalent variants matching the orientation [20]:

(1) $[1\bar{1}1]_f \parallel [110]_s$, $[\bar{1}12]_f \parallel [\bar{1}10]_s$,
(2) $[1\bar{1}1]_f \parallel [110]_s$, $[\bar{1}12]_f \parallel [\bar{1}\bar{1}0]_s$,
(3) $[1\bar{1}1]_f \parallel [\bar{1}10]_s$, $[\bar{1}12]_f \parallel [110]_s$,
(4) $[1\bar{1}1]_f \parallel [\bar{1}10]_s$, $[\bar{1}12]_f \parallel [\bar{1}\bar{1}0]_s$,

where the indices 'f' and 's' denote the film and the substrate, respectively. This has the result that in Mn–O–Mn–O–$\cdots$ chains angles of 19.5, 70.5, and 90° are formed on transition from one

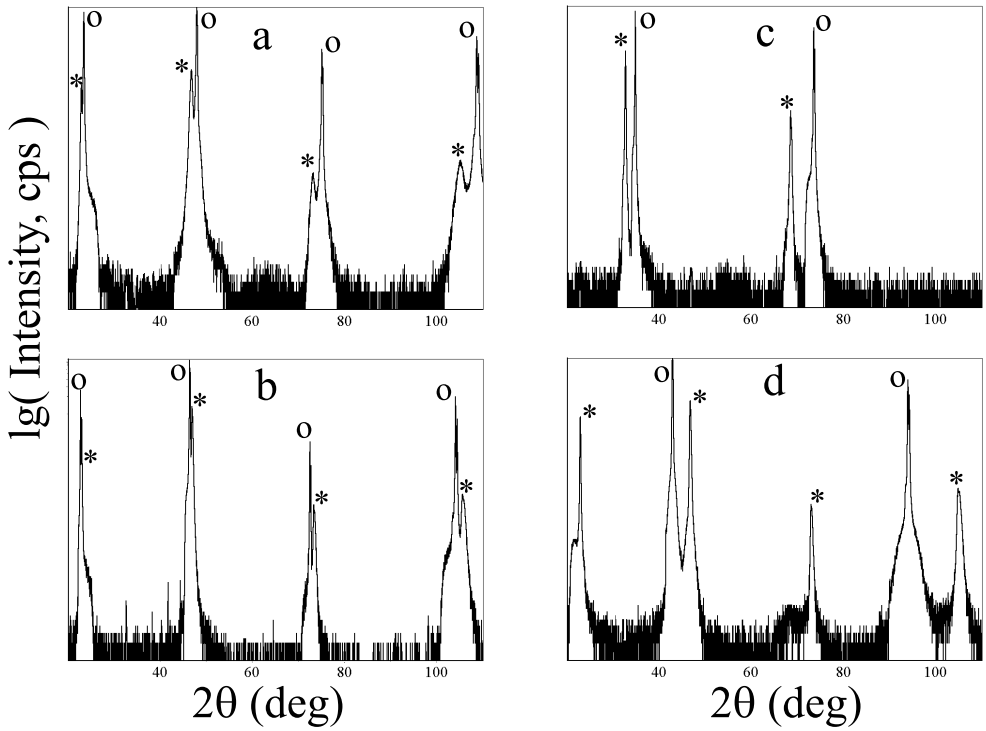


**Figure 1.** XRD diffraction patterns of the films on: (a) $LaAlO_3$; (b) $SrTiO_3$; (c) $ZrO_2(Y_2O_3)$; (d) MgO.

to another of the microregions having the different crystallographic orientations listed above. Such an orientation observed also for the films of $La_{1-x}Sr_xMnO_3$ [18], $La_{1-x}Na_xMnO_{3-\delta}$ [20], and $(La, Pr)_{0.7}Ca_{0.3}MnO_3$ [21] results in the formation of a nanoscale domain structure with an extremely high density of boundaries. The pseudocubic (110) reflections were not split for $La_{0.35}Nd_{0.35}Sr_{0.3}MnO_3$ films on $ZrO_2(Y_2O_3)$. Similar behaviour is known for orthorhombic $(La, Pr)_{0.7}Ca_{0.3}MnO_3$ but not for rhombohedral $La_{1-x}Na_xMnO_3$ films on $ZrO_2(Y_2O_3)$.

The lattice parameters were calculated from a set of measured out-of-plane reflections. The lattice parameters found are very close to those of the pseudocubic structure (table 2). The in-plane lattice parameters cannot be further resolved. In fact, at room temperature, $La_{0.35}Nd_{0.35}Sr_{0.3}MnO_3$ with the mean ionic radius of the A cation equal to 1.225 Å (tolerance factor $t = 0.922$) is expected to be nearly at the morphotropic boundary of the orthorhombic *Pnma* and rhombohedral *R*3*c* structures [22]. Reflections other than that of the simple perovskite structure were not observed for the $La_{0.35}Nd_{0.35}Sr_{0.3}MnO_3$ samples. A possible reason could be too small a magnitude of the lattice distortion near to the morphotropic boundary. The XRD pattern of the bulk material at room temperature was described in the rhombohedral group with the lattice parameters $a = 5.488(4)$ Å and $c = 13.392(7)$ Å (hexagonal setting) which is very close to the cubic structure ($a\sqrt{6}/c = 1.004$). Also the difference between the lattice parameters for the films on different substrates is very small. In particular, the volume of the perovskite cell is nearly constant.

Thus the lattice strain typical for thin films of the perovskite manganites seems to be nearly relaxed in the $La_{0.35}Nd_{0.35}Sr_{0.3}MnO_3$ films and its influence on the physical properties can be neglected. The lattice parameters of the film on $ZrO_2(Y_2O_3)$ calculated from the observed

**Table 2.** Magnetic, electrical, and structural characteristics of $La_{0.35}Nd_{0.35}Sr_{0.3}MnO_3$ films.

| Characteristics | MgO | $LaAlO_3$ | $SrTiO_3$ | $ZrO_2(Y_2O_3)$ |
|---|---|---|---|---|
| Curie temperature $T_C$ (K) ($H = 10$ Oe) | 242 | 231 | 219 | |
| Curie temperature $T_C$ (K) ($H = 100$ Oe) | | 241 | 223 | 245 |
| Magnetic moment, $M$ ($\mu_B$/formula unit) | 1.7 | 1.6 | 2 | 1.9 |
| $T_{max}$ (K)—temperature of maximum resistivity $\rho$ | 252 | 252 | 252 | 225 |
| $T_{min}$ (K)—temperature of minimum magnetoresistance $\Delta\rho/\rho$ ($H = 8.4$ kOe) | 228 | 223 | 213 | 225 |
| $\rho_{max}$ ($\Omega$ cm), maximum $\rho$ | 0.085 | 0.13 | 0.084 | 0.63 |
| $\rho_{82\,K}$ ($\Omega$ cm), value of $\rho$ at 82 K | 0.0089 | 0.0059 | 0.0040 | 0.19 |
| $\lvert\Delta\rho/\rho\rvert_{max}$—maximum magnetoresistance magnitude ($H = 8.4$ kOe) in the $T_C$-region | 0.34 | 0.23 | 0.22 | 0.13 |
| $\lvert\Delta\rho/\rho\rvert_{82\,K}$ ($T = 82$ K, $H = 8.4$ kOe) | 0.04 | 0.03 | 0.03 | 0.11 |
| Film orientation | (001) | (001) | (001) | (110) |
| Film thickness (Å) | 4100 | 5500 | 5500 | 5500 |
| Out-of-plane parameter (Å) | $3.882 \pm 0.001$ | $3.880 \pm 0.002$ | $3.872 \pm 0.001$ | $3.874 \pm 0.001$ |
| In-plane parameter (Å) | $3.876 \pm 0.002$ | $3.875 \pm 0.002$ | $3.878 \pm 0.001$ | $3.881 \pm 0.002$ |
| Perovskite cell volume (Å$^3$) | $58.32 \pm 0.08$ | $58.26 \pm 0.09$ | $58.23 \pm 0.05$ | $58.25 \pm 0.06$ |

out-of-plane reflections are close those of the films on the perovskite substrates (table 2). Thus, we can conclude that the $La_{0.35}Nd_{0.35}Sr_{0.3}MnO_3$ thin-film samples prepared on the different substrates possess practically the same crystal structure but different microstructures.

*3.1.2. Scanning electron microscopy.* The surface morphology of the films was rather smooth. No cracks or voids could be detected on the surfaces of the films. The surface of each film was formed of hillocks of average lateral size 0.5–1 $\mu$m. Such morphology is typical for perovskite manganite films $\sim$0.5 $\mu$m thick grown by MOCVD [19]. The surface of the films on $ZrO_2(Y_2O_3)$ was smoother than that of the films on the perovskite substrates (figure 2). Numerous terraces were observed on the surface of the film on MgO substrate. The terraces originate from the substrate surface morphology typical for MgO [23, 24].

*3.1.3. High-resolution electron microscopy.* The film–substrate interfaces both for the films on $SrTiO_3$ and on $LaAlO_3$ and for the film on MgO were free of any products of possible chemical interaction between the film and the substrate. The interface with the perovskite substrate was found coherent and atomically flat. The film–substrate lattice mismatch is relieved by the formation of misfit dislocations at the interface. The density of the misfit dislocations correlates with the lattice mismatch magnitude (figure 2): 0.8% with $SrTiO_3$, 2% with $LaAlO_3$, and 8% with MgO. The results are in agreement with XRD data revealing the relaxation of the film–substrate mismatch.

Electron diffraction (ED) patterns reveal a subtle difference between the films on $SrTiO_3$ and MgO. Normally, the ED patterns of the films are overlapped by the contribution of the substrate (figure 2). In the case of the film on MgO the reflections of the film and the substrate

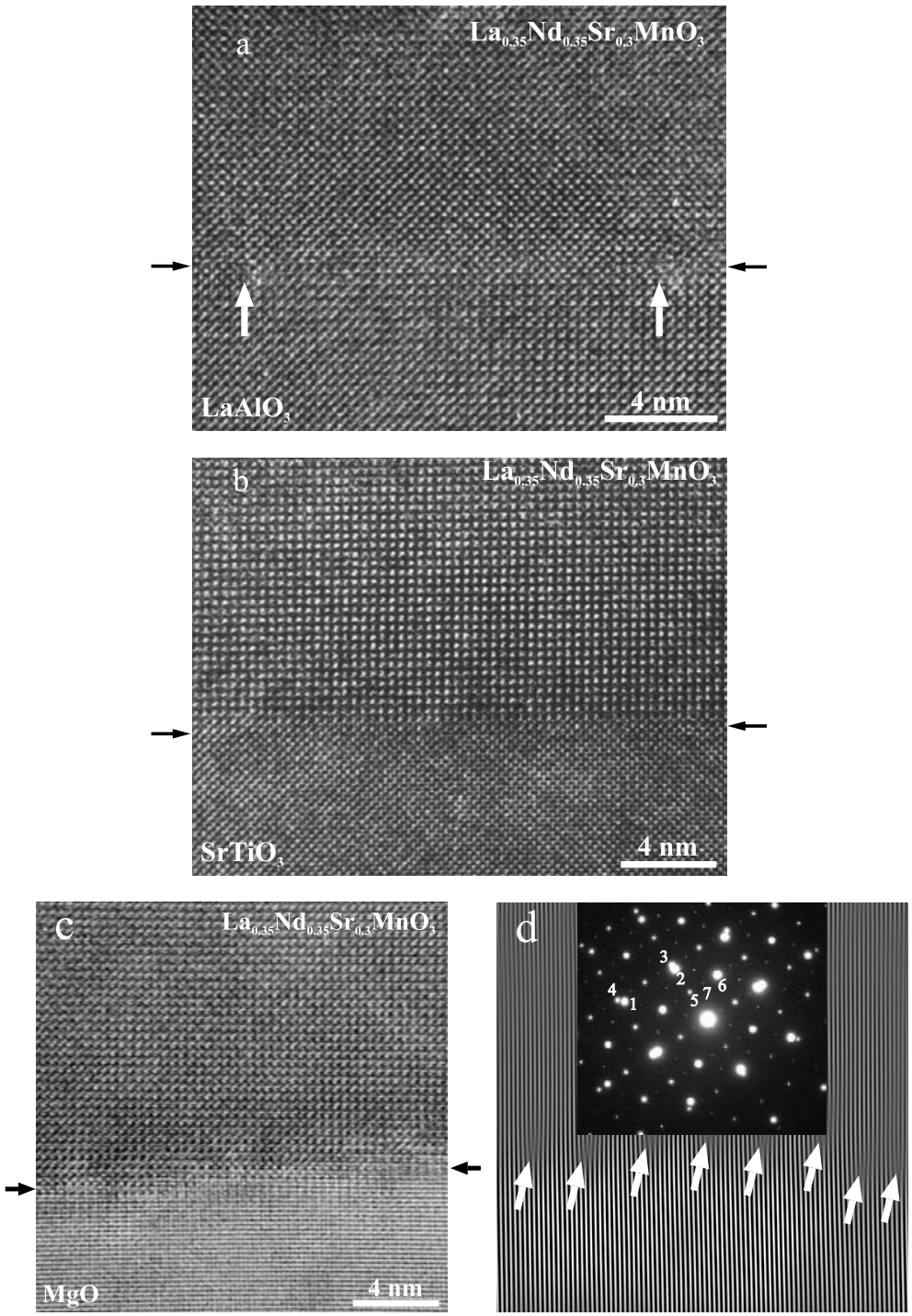


**Figure 2.** The film–substrate interfaces according to the HREM study: (a) the film on $LaAlO_3$; (b) the film on $SrTiO_3$; (c) the film on MgO; (d) the ED pattern with the cell doubling for the film on MgO. The black arrows denote the interface; white arrows denote the misfit dislocation core.

can be easily distinguished due to the large difference in lattice parameters and systems of extinction. Besides the reflections of the simple perovskite lattice, a set of superstructural reflections is clearly observed. They imply unit-cell doubling along the [001] direction. The observed reflection is a signature of orthorhombic symmetry [25].

In the case of the films on the perovskite substrates, the ED patterns of the film and substrate overlap. Nevertheless, because $SrTiO_3$ is a cubic perovskite and $LaAlO_3$ is a rhombohedrally distorted perovskite, the overlap does not mask the orthorhombic superstructure in the film. We have found many areas in the films where no doubling was detected. At the same time, the ED from areas large compared with the film thickness always contained additional reflections corresponding to the doubling. There are two possible explanations for this behaviour.

First, orthorhombic twins could be present in the film with the doubling axes oriented in the orthogonal directions, thus providing no visible doubling for some of the twins. But the lattice distortion is too small for detecting the individual twins or twin boundaries.

Another explanation could be that the film on the perovskite substrate with cubic or rhombohedral symmetry is closer to the morphotropic boundary or even partly in the rhombohedral state. Probably the residual epitaxial strain is responsible for the difference. According to [22], crossing over the morphotropic boundary has no step-like effect on the electrical and magnetic properties of the perovskite manganites. Our results discussed below are in agreement with this conclusion. It is noteworthy that transition over the morphotropic boundary is possible when the temperature decreases.

An interesting extended structural defect was found in $La_{0.35}Nd_{0.35}Sr_{0.3}MnO_3$ films on perovskite substrates. This defect can be considered as an intergrowth of the $K_2NiF_4$-type structure with the original perovskite structure. The extra planes containing A cations of the perovskite structure were found to be extended both along and across the film. The layers inserted along the film plane were found to be extended over the whole region available for the high-resolution observations (a few $\mu$m). The observation is evidence for 2D nucleation rather than 3D nucleation during the epitaxial growth on the low-mismatch substrate $SrTiO_3$. The intergrowths imply a deviation of the cation ratio from the stoichiometric value. But the volume occupied by the intergrowth is very small and corresponds to less than 1% deviation of the cation stoichiometry. Thus, it cannot be controlled by routine EDX analysis. It is noteworthy that neither orthorhombic $(La, Pr)_{0.7}Ca_{0.3}MnO_3$ not rhombohedral $La_{1-x}Na_xMnO_3$ demonstrate such intergrowths with the same composition control. Thus, doping with Sr is necessary to stabilize the intergrowths. Because of the low concentration in the sample, we cannot expect any strong effect of the intergrowths on the magnetic and electrical properties of the films.

### *3.2. Magnetic properties*

The magnetization $M$ of the films was measured in a magnetic field $\boldsymbol{H}$ applied parallel to the plane of the film and corrections to the magnetization of the substrate were introduced. Figure 3 gives the dependence $M(H)$ for all the films at $T = 5$ K. It can be seen that the magnetization of all the films, except that on MgO, saturates rapidly in a field of a few kilo-oersteds. For the film on MgO, saturation in the range 7–25 kOe is followed by an almost linear increase in $M$ with further increasing field (the maximum measured field is $H = 50$ kOe) and the magnetic moment per chemical formula unit increases from 1.7 $\mu_B$ to 1.8 $\mu_B$. The limiting hysteresis loops of all the films are fairly narrow and the coercive force does not exceed 300 Oe. Curves of the temperature dependence of the initial magnetic susceptibility $M/H$ ($H = 10$ and 100 Oe) were used to determine the Curie point $T_C$ by extrapolating the steepest part of the curves $(M/H)(T)$ to the intersection with the temperature axis. The values of $T_C$ for all the films studied here are given in table 2.

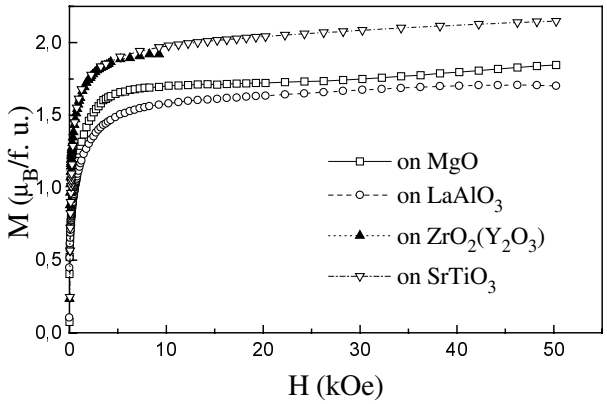


**Figure 3.** The dependence of the magnetization $M$ of $La_{0.35}Nd_{0.35}Sr_{0.3}MnO_3$ thin films on various substrates on the magnitude of the magnetic field $\boldsymbol{H}$ parallel to the surface of the film at $T = 5$ K.

### *3.3. Electrical properties*

Figure 4 gives the temperature dependence of the electrical resistivity $\rho$ for all the films studied. Figure 5 gives the temperature dependence of the magnetoresistance $\Delta\rho/\rho = (\rho_H - \rho_{H=0})/\rho_H$ for the films on $SrTiO_3$ and $ZrO_2(Y_2O_3)$. Figures 6 and 7 show $\Delta\rho/\rho$ isotherms at various temperatures for these films. The $(\Delta\rho/\rho)(T)$ and $(\Delta\rho/\rho)(H)$ curves for films on MgO and $LaAlO_3$ are similar to those plotted in figures 5(a) and 6(a) for films on $SrTiO_3$. It can be seen from figures 5, 6, and 7 that the magnetoresistance is negative. Our studies showed that the magnitude and sign of $\Delta\rho/\rho$ do not depend on the direction of the electric current density in the plane of the film nor on the angle between this direction and the direction of the magnetic field, i.e. magnetoresistance is isotropic in the plane of the film. The temperatures of the maxima in the curves $\rho(T)$ and the minima in the curves $(\Delta\rho/\rho)(T)$ are given in table 2 for all the films studied.

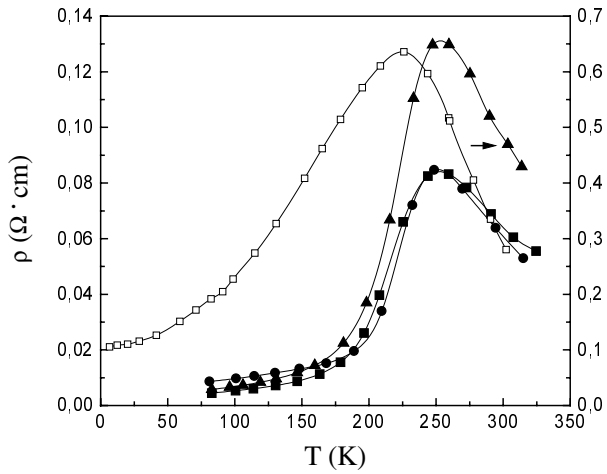


**Figure 4.** Temperature dependences of the electrical resistivity $\rho$ of $La_{0.35}Nd_{0.35}Sr_{0.3}MnO_3$ thin films on various substrates: (open squares) $ZrO_2(Y_2O_3)$; (solid squares) $SrTiO_3$; (solid circles) MgO; (solid triangles) $LaAlO_3$.

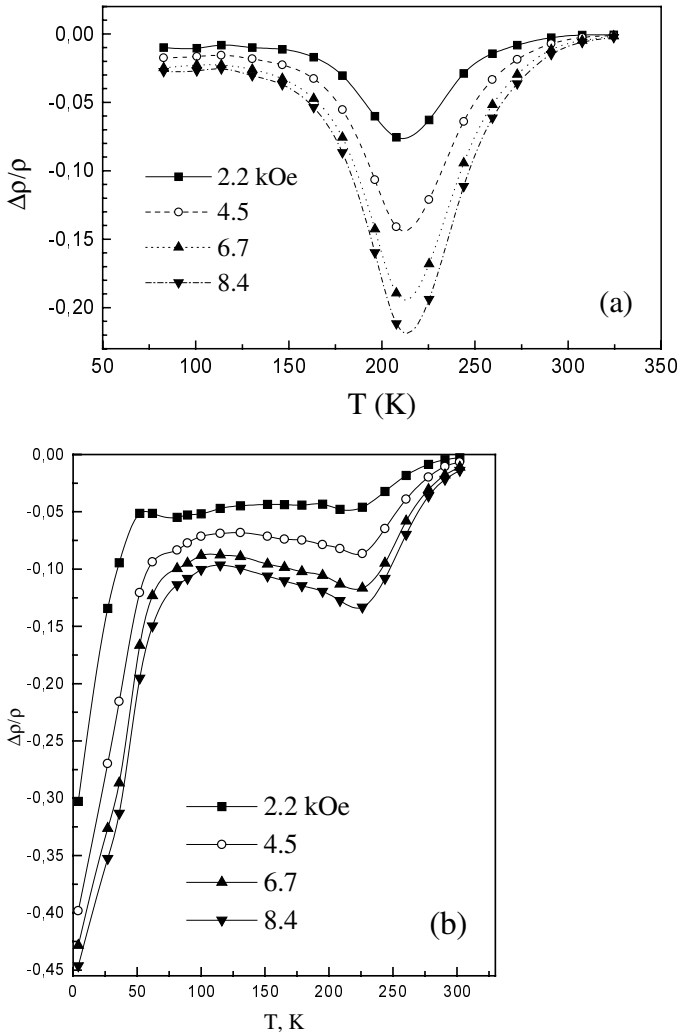


**Figure 5.** Temperature dependences of the magnetoresistance $\Delta\rho/\rho$ of $La_{0.35}Nd_{0.35}Sr_{0.3}MnO_3$ thin films on (001)$SrTiO_3$ (a) and (001)$ZrO_2(Y_2O_3)$ substrates (b).

## 4. Discussion and results

It can be seen from figure 4 that the curves of $\rho(T)$ have a maximum and, as can be seen from table 2, the temperature $T_{max}$ at the maximum of $\rho(T)$ for the film on $ZrO_2(Y_2O_3)$ is 20 K lower and that for the films on $SrTiO_3$, $LaAlO_3$, and MgO is approximately 20 K higher than $T_C$. The magnetoresistance is negative and the curves $(\Delta\rho/\rho)(T)$ pass through a minimum near $T_C$ (figure 5). The isotherms of the magnetoresistance do not saturate over the entire temperature range studied (figures 6, 7). The magnetoresistance in the $T_C$-region reaches 34% at $H = 8.4$ kOe for the film on MgO and is lower for the other films, being 23%, 22%, and 13% for films on $SrTiO_3$, $LaAlO_3$, and $ZrO_2(Y_2O_3)$, respectively (see table 2). Thus, for these films we observe colossal magnetoresistance near $T_C$ similar to that obtained in manganites of different compositions [26–28].

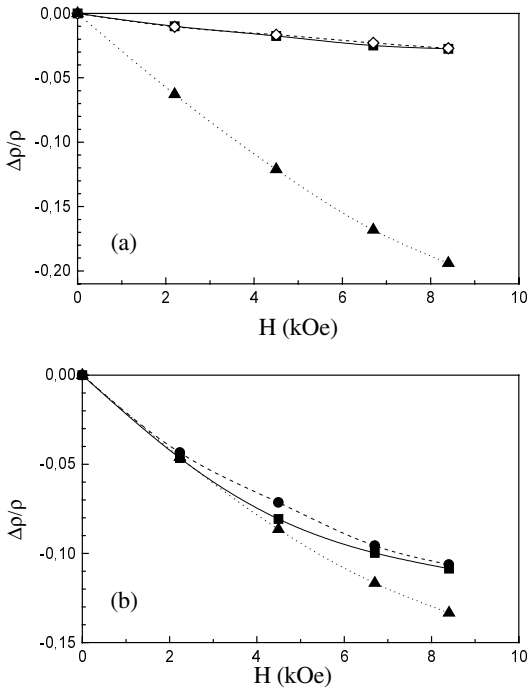


**Figure 6.** Isotherms of the magnetoresistance $\Delta\rho/\rho$ of $La_{0.35}Nd_{0.35}Sr_{0.3}MnO_3$ thin films on (001)$SrTiO_3$ (a) and (001)$ZrO_2(Y_2O_3)$ substrates (b) at $T = 82$ K (solid squares), 100 K (open diamonds), 152 K (solid circles), and 225 K (solid triangles).

A comparison of the $\rho(T)$ curves for the film on the $ZrO_2(Y_2O_3)$ substrate and the other three films on the perovskite and MgO substrates (figure 4) shows that the value of $\rho$ for the first film is much higher than those for the others. It can be seen from table 2 and figure 4 that the resistivities differ by more than an order of magnitude and near the maximum of $\rho$ they differ by factors between four and eight. The forms of the curves also differ. For example, for the films on $SrTiO_3$, MgO, and $LaAlO_3$, $\rho$ increases abruptly with increasing temperature from $T = 180$ K, whereas for the film on $ZrO_2(Y_2O_3)$, $\rho$ begins to increase monotonically from 4.2 K, i.e., the maximum in the $\rho(T)$ curve is broadened substantially. The $(\Delta\rho/\rho)(T)$ curves differ even more strikingly: for the first three films we observe an abrupt minimum at $T_{min}$ which is slightly lower than $T_C$, whereas for the last film this minimum, also positioned slightly below $T_C$, is strongly broadened and is barely observed on the low-temperature side (figure 5). The value of $|\Delta\rho/\rho|$ for the last film at low temperatures is high, reaching almost 12% in a field of 8.4 kOe for $100 \leqslant T \leqslant 240$ K, and from 100 K it increases strongly with further decrease in temperature. At 4.2 K this value reaches 45%. The $(\Delta\rho/\rho)(H)$ curves (figures 6, 7) for the first three films and the last one differ substantially: for the first three films we observe an almost linear increase in $|\Delta\rho/\rho|$ with increasing field at temperatures below the minimum of the $(\Delta\rho/\rho)(T)$ curve, whereas for the last film in a weak field up to 2 kOe we observe an abrupt increase in $|\Delta\rho/\rho|$ followed by an almost linear increase in $|\Delta\rho/\rho|$ in stronger fields.

The dependences ($\rho(T)$, $(\Delta\rho/\rho)(H)$, and $(\Delta\rho/\rho)(T)$) described above for the film on $ZrO_2(Y_2O_3)$ are similar to those observed earlier for polycrystalline bulk and thin-film manganese samples [3–17], whereas the dependences observed for the films on $SrTiO_3$,

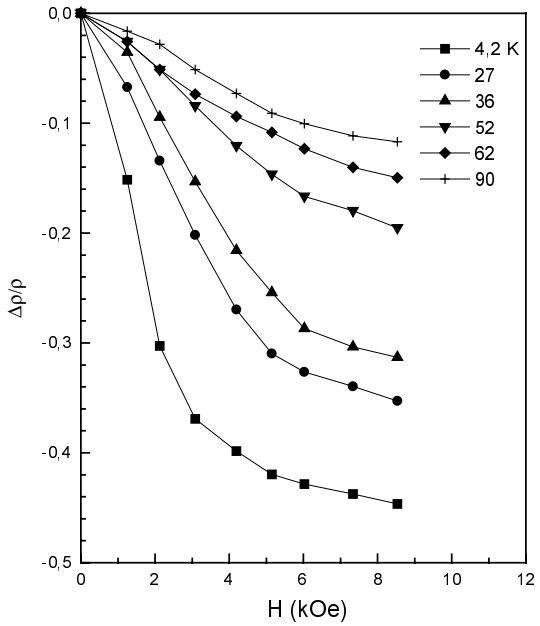


**Figure 7.** Isotherms of the magnetoresistance $\Delta\rho/\rho$ of $La_{0.35}Nd_{0.35}Sr_{0.3}MnO_3$ thin films on (001)$ZrO_2(Y_2O_3)$ substrates at low temperature.

$LaAlO_3$, and MgO are similar to those observed for single-crystal samples [3–17]. The enhanced value of $\rho$ in the polycrystalline samples can be attributed to spin-polarized tunnelling between granules [9] or scattering of charge carriers within domain walls which generally coincide with the intergranular boundaries [4], whereas the enhanced values of $|\Delta\rho/\rho|$ at $T < T_C$ can be ascribed to the influence of the magnetic field on the processes. It was shown in [29] that the nuclear resonance data for an $La_{0.67}Ca_{0.33}MnO_3$ film indicate a reduced hole concentration within the domain walls.

However, all the films studied here are epitaxial, including that on $ZrO_2(Y_2O_3)$. The difference between this film and the others studied here is that, as we noted in section 3.1.1, it consists of microregions having four different crystallographic orientations. This leads to the existence of magnetic domains having at least four different directions of easy-magnetization axes, and the boundaries between them form different angles with the directions of magnetization in the domains. In films on perovskite and MgO substrates the axes of easy magnetization of their different parts are parallel and thus most of the film should be occupied by magnetic domains having 180° walls.

It can be seen from the values of $\rho$ at $T < T_C$ for films on perovskite and MgO substrates (table 2) that their conductivity is of metallic type. From this it follows that exchange via charge carriers, i.e., holes, predominates in $La_{0.35}Nd_{0.35}Sr_{0.3}MnO_3$. The Curie temperature in this case is given by [30]

$$T_C \propto ztv \tag{1}$$

where $t$ is the transport integral (the width of the conduction band $W$ is proportional to $t$), $z$ is the coordination number of the magnetic ion (Mn in this case), and $v$ is the number of charge carriers per magnetic ion. It can be seen from table 2 that the Curie temperature of the film on $ZrO_2(Y_2O_3)$ is approximately the same as that for the other film. This implies that exchange via the charge carriers, i.e., holes, also takes place for this film and the increase

in its electrical resistivity by more than an order of magnitude compared with those of the three other films is attributable to the boundaries between the regions having different crystallographic orientations. It has been noted that the other three films studied here do not have such boundaries. In this case, the electrical resistivity of the film on $ZrO_2(Y_2O_3)$, as in polycrystalline samples, consists of two components: the electrical resistivity $\rho_1$ within the crystallographic regions described in section 3.1.1 having an average linear dimension $L$ (or the electrical resistivity within isolated granules in the case of polycrystal), i.e., the intrinsic electrical resistivity of the material, and the resistivity $\rho_2$ within the boundaries between regions of different crystallographic orientation, having the average thickness $L'$ (or the electrical resistivity of the intergranular boundaries). The value of $\rho$ is written in the form [31]

$$\rho = \rho_1 + (L'/L)\rho_2. \tag{2}$$

In the film on $ZrO_2(Y_2O_3)$, boundaries exist between the regions of different crystallographic orientation, the angles between these being 19.5°, 70.5°, and 90°. This implies that the angles $\theta$ in the Mn–O–Mn–O–Mn–$\cdots$ chains between lines connecting two manganese ions with an oxygen ion, which are close to 180° within the crystallographic regions, change abruptly to the values given above within the boundaries between these microregions.

We know that the width of the conduction band in manganites (single-electron approximation) is proportional to $\cos^2\theta$ [28], so an abrupt decrease in $\theta$ within the boundary between microregions of different crystallographic orientation leads to a sharp drop in conductivity within this boundary. Electron microscopy of this film has shown that the thickness of the boundary is close to the lattice constant (∼4 Å) [32]. However, all the sections of the films on $SrTiO_3$, $LaAlO_3$, and MgO have the same crystallographic orientation and do not exhibit these boundaries. Consequently the increase in $\rho$ in the film on $ZrO_2(Y_2O_3)$ is only attributable to the second term in expression (2). Assuming that the value of $\rho_1$ is the same for all four films and is approximately $6 \times 10^{-3}$ Ω cm (table 2), and substituting the values $L' = 4$ Å and $L \simeq 400$ Å [32] into expression (2), we find that $\rho_2 \simeq 18.4$ Ω cm at 82 K. Hence, the electrical resistivity inside the boundary between microregions of different crystallographic orientation is more than three orders of magnitude higher than that inside the microregions and is of the same order of magnitude as in semiconductors.

The small thickness of the boundary layer and the high value of $\rho_2$ suggest that the conduction here is achieved by tunnelling through this boundary. It will be shown that some of these boundaries coincide with the domain walls. In this case, the tunnelling has a specific feature associated with the fact that almost completely spin-polarized electrons tunnel. This case was described in [9] for polycrystalline bulk manganese samples. When the electron spin is conserved during tunnelling and the magnetic moments of neighbouring granules are not parallel, the magnetoresistance is described by the following expression [6]:

$$\frac{\Delta\rho}{\rho} = -\frac{JP}{4k_BT}[m^2(H,T) - m^2(0,T)] \tag{3}$$

where $J$ is the intergranular exchange constant, $P$ is the electron polarization, and $m$ is the magnetization normalized to the saturation value. This expression can evidently be used for the film on $ZrO_2(Y_2O_3)$. It can be seen from expression (3) that when technical saturation of the magnetization is reached, the absolute value of the magnetoresistance should also saturate.

However, figures 6, 7 show that for the film on $ZrO_2(Y_2O_3)$ no saturation is observed in the magnetoresistance isotherms at low temperatures although saturation of the magnetization had already been achieved (see figure 3). It can be seen from figures 6, 7 that at low temperatures the magnetoresistance isotherms initially show an abrupt increase in $|\Delta\rho/\rho|$ in fields up to 2 kOe which is followed by a slower almost linear increase with further increasing

$H$. Thus, we should assume that in addition to the spin-polarized tunnelling noted above, some other processes are also partly responsible for the low-temperature magnetoresistance in fields exceeding the technical saturation field.

We have already noted that the enhanced low-temperature electrical resistivity and magnetoresistance in polycrystalline samples has also been attributed to scattering of the charge carriers caused by disordering of the spin system inside the domain walls. However, this explanation is hardly applicable to manganites for which strong s–d exchange takes place and the domain wall thickness is considerable. It was noted in section 3.2 that the coercive force is approximately 300 Oe in all these films. It follows from figure 3 that the saturation magnetization is $M = 300$ G for all the films. The effective magnetic anisotropy constant calculated from these data is $K_{eff} = 9 \times 10^4$ erg cm$^{-3}$. Hence the films considered here possess low magnetic anisotropy which is typical of manganites [33], so the domain wall thickness is large. According to estimates [34] for similar magnetically soft materials, it may reach $10^3a$ ($a$ is the lattice constant) in bulk samples.

In thin-film samples, where the film thickness is of the same order as the domain wall thickness indicated for a bulk sample (the thickness of the films considered here is 4100–5000 Å), the domain structure is more complex. At present there is no consensus as regards its structure [34]. Thus, as a rough approximation we assume that the domain wall thickness in thin films is the same as in the bulk sample. As has been noted, the size of the crystallographic microregions in the film on $ZrO_2(Y_2O_3)$ is an order of magnitude smaller than the smallest possible domain wall thickness. Since long-range magnetic order is achieved in the film, each magnetic domain should contain more than ten crystallographic microregions. However, in some parts of the film long-range magnetic order may be absent because the domain wall thickness is larger than the size of the crystallographic microregions and is of the same order as the film thickness. It can be seen from figure 3 and table 2 that the magnetic moment per chemical formula unit for this film is severely diminished compared with that predicted for the complete ferromagnetic ordering of all the ions (including the magnetic sublattice of $Nd^{3+}$ ions) and is approximately 46% of this. In such a wide domain wall, spin turning takes place gradually, and as a result of the strong s–d exchange the carrier spin is aligned parallel to the spin of the ion at which it is located at any given moment and the charge carrier is not scattered [30].

It can be seen from figure 5 that the $(\Delta\rho/\rho)(T)$ curves have a minimum near $T_C$ for all four films studied. The absolute value of $\Delta\rho/\rho$ at the minimum $|\Delta\rho/\rho|_{max}$ is high: 34% for the film on MgO and 13% for the film on $ZrO_2(Y_2O_3)$; for the other two films we have 22.5% in a field of 8.4 kOe (table 2). For comparison we should note that in ordinary magnetic substances such as ferrites, the value of $|\Delta\rho/\rho|_{max}$ near $T_C$ is two or three orders of magnitude lower. The compound $La_{0.35}Nd_{0.35}Sr_{0.3}MnO_3$ is a strongly strontium-doped antiferromagnetic semiconductor $La_{0.5}Nd_{0.5}MnO_3$ in which metallic conductivity is observed below $T_C$ and a transition to semiconducting conductivity take place near $T_C$ (see figure 4). It was shown in [35] that in manganites of this type with strong s–d exchange there are two mechanisms by which impurity–magnetic carrier interaction influences the resistance: carrier scattering which reduces their mobility and the formation of localized states near the top of the valence band. Near $T_C$ the carrier mobility drops sharply and the charge carriers are partially localized at levels near the top of the valence band. Under the action of a magnetic field the impurity–magnetic carrier scattering diminishes and the carriers delocalize from the tail of the valence band.

It can be seen from figure 5(b) that for the film on $ZrO_2(Y_2O_3)$ the minimum in the $(\Delta\rho/\rho)(T)$ curve near $T_C$ is barely distinguishable and the value of $|\Delta\rho/\rho|$ in the low-temperature range up to 100 K is only 2–3% lower than that near $T_C$. This suggests that the natures of the magnetoresistance at low temperatures in fields above the technical saturation

of the magnetization and near $T_C$ are the same. At low temperatures in spin-disordered microregions occupying around 54% of the film area in which the charge carriers are situated under approximately the same conditions as near $T_C$, the spins are strongly disordered and strong s–d exchange takes place. However, this is only possible when the spin-disordered regions exist in fields higher than the technical saturation of the magnetization.

We can explain the behaviour of the low-temperature magnetoresistance in fields above the technical saturation level in films on $SrTiO_3$, $LaAlO_3$, and MgO substrates in the same fashion as for films on $ZrO_2(Y_2O_3)$, since the first three films also contain spin-disordered microregions. This is evidenced by the excessively low saturation magnetizations of films on $SrTiO_3$, $LaAlO_3$, and MgO compared with the pure spin value for ferromagnetic ordering of all the ions (see table 2 and figure 3). It can be seen from figure 3 that for the film on MgO after saturation in fields between 10 and 25 kOe, the magnetic moment increases almost linearly with the field. We know that as a result of mismatch between the crystal structures of the material and the substrate, manganite films exhibit stresses which increase the magnetic anisotropy. However, the stresses in films on a MgO substrate relax rapidly. As was noted in section 3.1.1, in films having this composition the stresses are very weak because this composition is positioned near the morphotropic boundary between the orthorhombic and rhombohedral structures which further intensifies the relaxation of the film on MgO. This film is clearly the least stressed of all those studied and thus the field-induced spin ordering in magnetically disordered microregions takes place in it at field $H > 25$ kOe.

By replacing Nd with La in $Nd_{0.7}Sr_{0.3}MnO_3$ we hoped to increase the Curie temperature of the film. We based this hope on the following reasoning. We know that in an undistorted perovskite structure the Mn–O–Mn bond angle is 180°. When Nd ions are replaced with smaller Sr ions, the lattice becomes distorted. It could be predicted that partially replacing Nd ions with larger La ions will make the bond angle close to 180°, resulting in broadening of the conduction band, and thus increasing the transport integral $t$ and intensifying the exchange via the carriers. As a result, in accordance with expression (1), the Curie temperature increases. However, as can be seen from table 2, replacing half the Nd ions with La did not give the predicted result: the value of $T_C$, equal to 240 K for $Nd_{0.7}Sr_{0.3}MnO_3$ [36], remained the same for $La_{0.35}Nd_{0.35}Sr_{0.3}MnO_3$. This may be attributed to the crystallographic disordering of the A sites in $ABO_3$ perovskite described, for example, in [37]. As a result of this disordering, the orthorhombic distortion of the perovskite lattice in this last compound is the same as in the first, which leads to equal transport integrals $t$ in the two compositions and consequently to their Curie points being the same in accordance with expression (1).

## 5. Conclusions

We have described a new possibility for the existence of colossal magnetoresistance over a wide temperature range in manganites, and specifically in epitaxial thin films in which microregions having different crystallographic orientations exist. These epitaxial films differ from polycrystalline films in that they contain microregions of several types with different crystallographic orientations and they have an ordered configuration in the plane of the film. Since the crystallographic orientations in neighbouring microregions differ, boundaries exist between them at which the angles in Mn–O–Mn–O–$\cdots$ chains differ from 180°, so the electrical resistivity of these boundaries $\rho_2$ is strongly enhanced compared with $\rho_1$ within the microregions. The existence of this possibility is described for an $La_{0.35}Nd_{0.35}Sr_{0.3}MnO_3$ epitaxial film on $ZrO_2(Y_2O_3)$ substrate. The thickness of the boundaries between the microregions of different crystallographic orientation is 4 Å and the ratio $\rho_2/\rho_1$ is approximately $10^3$,

the conductivity within the microregions being metallic. The most probable mechanism for electrical conduction across these boundaries is charge-carrier (hole) tunnelling. In fields up to technical saturation, the magnetoresistance is explained by facilitation of the charge-carrier tunnelling by the magnetic field [6]. At the same time the epitaxial growth on the perovskite and MgO substrates is of one type and the formation of the such boundaries does not occur. Thus, it allows no significant tunnel magnetoresistance.

In contrast, the epitaxial growth on $ZrO_2(Y_2O_3)$ is of several types and produces a high density of the special above-described boundaries. These are different from the boundaries in the polycrystalline bulk materials because of (1) the much higher density and (2) the special boundaries being present instead of random boundaries. This makes the influence of the above-mentioned boundaries more effective and essentially more reproducible than in polycrystalline bulk materials.

An estimate of the effective magnetic anisotropy constant $K_{eff}$ showed that $K_{eff} = 9 \times 10^4$ erg cm$^{-3}$. This means that the thickness of the walls between the magnetic domains is very large ($\simeq 10^3 a$), of the same order as the film thickness and an order of magnitude larger than the dimensions of the microregions of different crystallographic orientation. This has the result that some regions of the film are magnetically disordered, as is evidenced by the approximately halved magnetic moment per chemical formula unit. As a result of the absence of long-range magnetic order in these microregions, we can assume that the nature of the magnetoresistance in them is the same as the nature of that near $T_C$. For instance, the existence of strong s–d exchange leads to impurity–magnetic carrier interaction which causes scattering of the carriers, reducing their mobility, and leads to the formation of localized states near the top of the valence band. Because of this, the mobility of the charge carriers is abruptly diminished and they are partially localized at levels near the top of the valence band over a wide temperature range. Under the action of a magnetic field, the impurity–magnetic carrier scattering of the charge carriers decreases and they become delocalized from levels near the top of the valence band.

A sharp increase in the magnetoresistance with field when technical magnetization has not yet been achieved can be attributed to the increase in a field of the spin-polarized tunnelling across boundaries between microregions of different crystallographic orientation which coincide with the domain walls. This process is mainly responsible for the colossal magnetoresistance in the range $4.2 \leqslant T \leqslant 100$ K. The magnetoresistance in fields below the technical saturation of the magnetization can hardly be attributed to scattering of the charge carriers caused by disordering of the spin system within domain walls whose thickness is very large. With such wide domain walls, spin turning takes place gradually and, as a result of the strong s–d exchange, the carrier spin is aligned parallel to the spin of that ion at which it is situated at a particular moment; in this case no carrier scattering occurs [30].

Spin-disordered microregions exist in films on $SrTiO_3$, $LaAlO_3$, and MgO substrates too, since their magnetic moments per chemical formula unit are reduced, being only 46% of the pure spin value. Spin-disordered microregions can exist in both bulk and thin-film polycrystalline manganite samples too, provided that the dimensions of some of the crystallites do not exceed the domain wall thickness.

## Acknowledgments

This work was partly supported by INTAS (grants No 97-open-30253 and No 97-0963), INTAS-RFBR (grant IR 97-11954) and the Russian Foundation for Basic Research (projects No 00-02-017810 and No 00-15-96625).

## References


[1] Jonker G H and Van Santen J H 1950 *Physica* **16** 337
[2] Searle C and Wang S 1970 *Can. J. Phys.* **48** 2023
[3] Ju H L, Gopalakrishnan J, Peng J L, Li Q, Xiong G C, Venkatesan T and Greene R L 1995 *Phys. Rev.* B **51** 6143
[4] Schiffer P, Ramirez A P, Bao W and Cheong S-W 1995 *Phys. Rev. Lett.* **75** 3336
[5] Gupta A, Gong G Q, Xiao G, Duncombe P R, Lecoeur P, Trouilloud P, Wang Y Y, Dravid V P and Sun J Z 1996 *Phys. Rev.* B **54** R15 629
[6] Hwang H Y, Cheong S-W, Ong N P and Batlogg B 1996 *Phys. Rev. Lett.* **77** 2041
[7] Shreekala R, Rajeswari M, Ghosh K, Gu J Y, Kwon C, Trajanovic Z, Boettcher T, Greene R L, Ramesh R and Venkatesan T 1997 *Appl. Phys. Lett.* **71** 282
[8] Mahesh R, Mahendiran R, Raychaudhuri A K and Rao C N R 1996 *Appl. Phys. Lett.* **68** 2291
[9] Park J-H, Chen C T, Cheong S-W, Bao W, Meigs G, Chakarian V and Idzeral Y U 1996 *Phys. Rev. Lett.* **76** 4215
[10] Raychaudhuri P, Nath T K, Nigam A K and Pinto R 1998 *J. Appl. Phys.* **84** 2048
[11] Vlakhov E S, Chakalov R A, Chakalova R I, Nenkov K A, Dorr K, Handstein A and Muller K-H 1998 *J. Appl. Phys.* **83** 2152
[12] Petrov D K, Gupta A, Kirtley J R, Krusin-Elbaum L and Gill H S 1998 *J. Appl. Phys.* **83** 7061
[13] Akther Hossain A K M, Cohen L F, Damay F, Berenov A, MacManus-Driscoll J, Alford N N, Mathur N D, Blamire M G and Evetts J E 1999 *J. Magn. Magn. Mater.* **192** 263
[14] Walter T, Dorr K, Muller K-H, Holzapfel B, Eckert D, Wolf M, Schlafer D, Schultz L and Grotzschel R 1999 *Appl. Phys. Lett.* **74** 2218
[15] Bar'yakhtar V G, Pogorilyi A N, Belous N A and Tovstolytkin A I 1999 *J. Magn. Magn. Mater.* **207** 118
[16] Ziese M, Sena S P and Blythe H J 1999 *J. Magn. Magn. Mater.* **202** 292
[17] Fu Yonglai and Ong C K 2000 *J. Magn. Magn. Mater.* **208** 69
[18] Gorbenko O Yu, Demin R V, Kaul A R, Koroleva L I and Szymczak R 1998 *Phys. Solid State* **40** 263
[19] Gorbenko O Yu, Graboy I E, Bosak A A, Amelichev V A, Ganin A Yu, Kaul A R, Wahl G and Zandbergen H W 1999 *J. Physique* IV **9** 659
[20] Bibes M, Gorbenko O Yu, Martinez B, Kaul A R and Fontcuberta J 2000 *J. Magn. Magn. Mater.* **211** 47
[21] Gorbenko O Yu, Kaul A R, Bosak A A, Graboy I E, Zandbergen H V, Svetchnikov V L, Babushkina N A, Belova L M and Kugel K I 2000 *Solid State Commun.* **114** 407
[22] Radaelli P G, Marezio M, Hwang H Y, Cheong S-W and Batlogg B 1996 *Phys. Rev.* B **54** 8992
[23] Grossley A, Johnston C, Sofield C J, Myhra S, Holt S A, Jones C F and Watson G S 1997 *Thin Solid Films* **292** 96
[24] Norton M G, Summerfelt S R and Carter C B 1990 *Appl. Phys. Lett.* **56** 2246
[25] Zandbergen H W and Jansen J 1999 *Ultramicroscopy* **80** 59
[26] Nagaev E L 1996 *Phys.–Usp.* **39** 781
[27] Ramirez A P 1997 *J. Phys.: Condens. Matter* **9** 8171
[28] Tokura Y and Tomioka Y 1999 *J. Magn. Magn. Mater.* **200** 1
[29] Papavassiliou G, Fardis M, Milia F, Pissas M, Kallias G, Niarchos D, Dimitropoulos C and Scherrer P 1998 *Phys. Rev.* B **58** 12 237
[30] Nagaev E L 1983 *Phys. Magn. Semicond.* 431
[31] Berger H 1961 *Phys. Status Solidi* **1** 739
[32] Bibes M, Gorbenko O, Martinez B, Kaul A and Fontcuberta J 2000 *J. Magn. Magn. Mater.* **209**
[33] Suzuki Y, Hwang H Y, Cheong S-W, Siegrist T, Van Dover R B, Asamitsu A and Tokura Y 1998 *J. Appl. Phys.* **83** 7064
[34] Hubert A 1974 *Theorie der Domanenwande in Geordneten Medien* (Berlin: Springer) p 306
[35] Nagaev E L 1996 *Phys. Lett.* A **211** 313
[36] Bokov V A, Grigoryan N A, Bryzhina M F and Tikhonov V V 1968 *Phys. Status Solidi* **28** 835
[37] Rodriguez L M and Attfield J P 1998 *Phys. Rev.* B **58** 2426